AGU PUBLICATIONS

JGR

Journal of Geophysical Research: Solid Earth

RESEARCH ARTICLE

10.1002/2016JB013508

Key Points:
- Magma underplating may have thickened the Gangdese crust ~20 km to ~58 km at 55-45 Ma
- The Gangdese crust reached a thickness of ~68 km at approximately 20-10 Ma as a result of tectonic shortening
- The Gangdese Mountains broadly attained an elevation of >4000 m at approximately 55-45 Ma due to isostatic uplift and slab breakoff

Supporting Information:
- Supporting Information S1

Correspondence to:
D.-C. Zhu,
dchengzhu@163.com;
dczhu@cugb.edu.cn

Citation:
Zhu, D.-C., Q. Wang, P. A. Cawood, Z.-D. Zhao, and X.-X. Mo (2017), Raising the Gangdese Mountains in southern Tibet, *J. Geophys. Res. Solid Earth*, *122*, doi:10.1002/2016JB013508.

Received 31 AUG 2016
Accepted 23 DEC 2016
Accepted article online 26 DEC 2016

Raising the Gangdese Mountains in southern Tibet

Di-Cheng Zhu[1,2], Qing Wang[1], Peter A. Cawood[3,4], Zhi-Dan Zhao[1], and Xuan-Xue Mo[1]

[1]State Key Laboratory of Geological Processes and Mineral Resources, and School of Earth Science and Resources, China University of Geosciences, Beijing, China, [2]CAS Center for Excellence in Tibetan Plateau Earth Sciences, Beijing, China, [3]School of Earth, Atmosphere and Environment, Monash University, Clayton, Victoria, Australia, [4]Department of Earth Sciences, University of St. Andrews, Saint Andrews, UK

Abstract The surface uplift of mountain belts is in large part controlled by the effects of crustal thickening and mantle dynamic processes (e.g., lithospheric delamination or slab breakoff). Understanding the history and driving mechanism of uplift of the southern Tibetan Plateau requires accurate knowledge on crustal thickening over time. Here we determine spatial and temporal variations in crustal thickness using whole-rock La/Yb ratios of intermediate intrusive rocks from the Gangdese arc. Our results show that the crust was likely of normal thickness prior to approximately 70 Ma (~37 km) but began to thicken locally at approximately 70–60 Ma. The crust reached (58–50) ± 10 km at 55–45 Ma extending over 400 km along the strike of the arc. This thickening was likely due to magmatic underplating as a consequence of rollback and then breakoff of the subducting Neo-Tethyan slab. The crust attained a thickness of 68 ± 12 km at approximately 20–10 Ma, as a consequence of underthrusting of India and associated thrust faulting. The Gangdese Mountains in southern Tibet broadly attained an elevation of >4000 m at approximately 55–45 Ma as a result of isostatic surface uplift driven by crustal thickening and slab breakoff and reached their present-day elevation by 20–10 Ma. Our paleoelevation estimates are consistent not only with the C–O isotope-based paleoaltimetry but also with the carbonate-clumped isotope paleothermometer, exemplifying the promise of reconstructing paleoelevation in time and space for ancient orogens through a combination of magmatic composition and Airy isostatic compensation.

1. Introduction

Tibet has the world's largest and highest plateau (Figure 1a) and the thickest continental crust (60–80 km) [*Yakovlev and Clark*, 2014] (Figure 1b). When and how the plateau achieved these features is one of the most intriguing issues in the Cenozoic history of our planet [e.g., *England and Searle*, 1986; *Harrison et al*., 1992; *Molnar et al*., 1993; *Wang et al*., 2008; *Yin and Harrison*, 2000; *Ding et al*., 2014]. Most researchers agree that the current high elevation of the southern plateau was attained by isostasy due to crustal thickening, which is in contrast to the northern plateau that is compensated by the removal of dense lithosphere mantle [e.g., *Molnar et al*., 1993; *Jiménez-Munt et al*., 2008]. However, whether this thickening was achieved in the Late Cretaceous or Cenozoic and the relative contributions of tectonic and magmatic processes in accounting for thickening remain unresolved [e.g., *Yin et al*., 1994, 1999; *Murphy et al*., 1997; *Kapp et al*., 2007; *Mo et al*., 2007; *Chung et al*., 2009; *Guan et al*., 2012; *Ji et al*., 2012].

Comparison between the compositions of recently emplaced intermediate continental calc-alkaline magmatic rocks and geophysically determined crustal thickness, as well as studies from global correlations and specific orogens, show that geochemical indices can be used to track quantitatively temporal variations of crustal thickness in continental arcs [*Chiaradia*, 2015; *Chapman et al*., 2015; *Profeta et al*., 2015]. An extended application of this approach in this paper to the Gangdese arc in southern Tibet (Figure 1a), and assuming Airy isostatic compensation, enables us to quantify the crustal thickness of the arc and reconstruct the spatial and temporal uplift history of the Gangdese Mountains.

2. Gangdese Arc and Samples

The Tibetan Plateau consists primarily of the Songpan–Ganzi flysch complex, Qiangtang Terrane, Lhasa Terrane, and the Himalayas (Figure 1b), separated from north to south by the Jinsha, Bangong–Nujiang, and Indus–Yarlung Zangbo Suture Zones, respectively [e.g., *Yin and Harrison*, 2000; *Zhu et al*., 2013]. The Lhasa Terrane in southern Tibet is the last geological block accreted to Eurasia in the Early Cretaceous [*Zhu et al*., 2016] before its collision with the northward drifting Indian continent in the early Cenozoic [e.g., *Zhu*

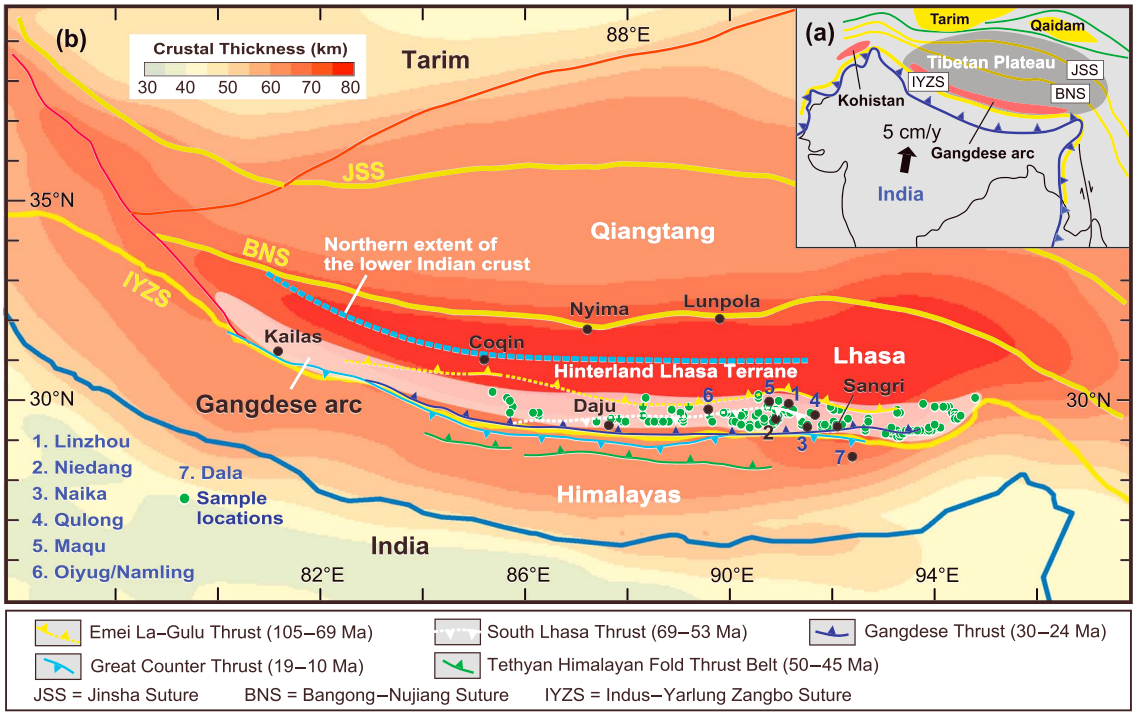

Figure 1. (a) Location of the Gangdese arc in the context of the Tibetan Plateau. (b) Simplified tectonic framework of the Tibetan Plateau and Himalayas, showing variations in crustal thickness [*Yakovlev and Clark*, 2014] and locations of samples compiled in this study. Locations of the Tethyan Himalayan Fold Thrust Belt [*Ratschbacher et al.*, 1994], Great Counter thrust and Gangdese thrust [*Yin et al.*, 1994, 1999], south Lhasa thrust and Emei La–Gulu thrust [*Murphy et al.*, 1997; *Kapp et al.*, 2007], and northern extent of the lower Indian crust [*Nábělek et al.*, 2009].

et al., 2015; *Hu et al.*, 2016]. Northward subduction of the Yarlung Zangbo Tethyan Ocean lithosphere along the southern margin of the Lhasa Terrane resulted in the development of a continental arc, now exposed as the voluminous Gangdese Batholith and Linzizong volcanic sequence (i.e., the Gangdese arc) [e.g., *Chung et al.*, 2005; *Zhu et al.*, 2013, 2015].

The intrusive rocks from the Gangdese arc (also termed the Gangdese or the Transhimalayan batholith) extend over 1500 km and vary between 20 and 60 km wide along the southern Lhasa Terrane (Figure 1b) [e.g., *Copeland et al.*, 1995; *Zhu et al.*, 2015]. These rocks were emplaced mostly from the Late Triassic (approximately 210 Ma) to the late Miocene (approximately 10 Ma) with two intense pulses of magmatic activity at 95–90 Ma and 52–48 Ma and a phase of widespread but volumetrically small felsic-dominated plutonism at 18–14 Ma (see Figure 2 and Table S1 in the supporting information for references). The pre-Cretaceous and Miocene rocks occur as small relics of varying size within the batholith. The widespread and volumetrically significant granitoids of early Paleogene age (60–45 Ma) are characterized by abundant mafic enclaves of similar age [e.g., *Ji et al.*, 2009; *Zhu et al.*, 2011, 2013]. The pre-Cretaceous and post-Cretaceous rocks are lithologically indistinguishable in the field. Samples used in this study are compiled from the well-studied central-eastern Gangdese Batholith (longitude E85°–E95°; Figure 1b). We expand on the *Zhu et al.* [2015] data by including calc-alkaline samples with zircon U-Pb ages between 210 Ma and 10 Ma (Table S1).

3. Methods and Results

Feldspar fractionation increases Rb/Sr ratio in felsic melts because Sr is compatible, whereas Rb is incompatible. Consequently, the elevated Rb/Sr ratio of samples can be used as an indicator of highly fractionated magmas [*Chapman et al.*, 2015]. Thus, to eliminate the effect of differentiation on primary magma composition, geochemical data used in this study were restricted to rocks in the range of 55 to 68 wt % SiO_2 (volatile free), with MgO values 1–6 wt % and Rb/Sr = 0.05–0.2. This filtering reduced the number of suitable samples from 830 to 203 (Table S2).

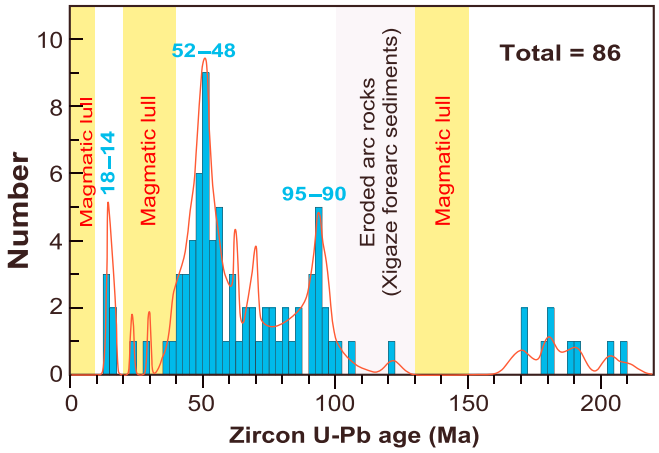

Figure 2. Histogram of crystallization ages (Ma) of the intrusive rocks (85–94°E) from the Gangdese arc. The red line represents the frequency curve. Age data used in this histogram are the crystallization ages defined by the youngest group of zircon analyses of each sample. To minimize sampling bias, only one age datum is selected for each pluton if (1) between-sample age difference is lower than 3 Myr and (2) the distance for sampling interval is less than ~15–10 km in longitude. This filtering reduced the number of samples with zircon U-Pb age from 281 to 86 (Table S1 in the supporting information) as shown in Figure 2.

High La/Yb and Sr/Y ratios of intermediate calc-alkaline rocks indicate the presence of garnet as a residual phase in the source [*Defant and Drummond*, 1990] because at high-pressure heavy rare earth elements and Y are preferentially partitioned into garnet. Melting of both subducted eclogitized oceanic crust [*Defant and Drummond*, 1990] and thickened eclogitized lower crust [*Chung et al*., 2003] can generate intermediate magmas with elevated La/Yb and Sr/Y ratios. Experimental studies on natural, hydrous basalts at 1–4 GPa show that the abundance of compatible elements (e.g., MgO, Ni, and Cr) in oceanic crust-derived melts will increase during ascent through the mantle wedge because the melts undergo metasomatic reactions with orthopyroxene and garnet in the mantle peridotite [*Rapp et al*., 1999; *Martin et al*., 2005]. As shown in Figure 3a, some of the 122–100 Ma high-Mg dioritic samples and the 96–82 Ma intermediate samples show high Ni abundances, plotting toward the field defined by the approximately 137 Ma oceanic crust-derived Mamen high-Mg adakitic rocks from the Gangdese arc [*Zhu et al*., 2009]. This trend corroborates that the two phases of magmatism are most likely derived from partial melting of the subducting Neo-Tethyan oceanic crust followed by interaction between slab-derived melt and mantle wedge peridotite [*Ma et al*., 2013]. Therefore, the 122–100 Ma high-Mg dioritic samples and the 96–82 Ma intermediate samples from the Gangdese Batholith are excluded for tracking crustal thickness.

Crustal thickness in the Andean convergent margins correlates with geochemical indices of arc lavas [*Plank and Langmuir*, 1988; *Haschke et al*., 2002]. This correlation was corroborated and formulated by examining geophysically determined crustal thickness (Moho depth) and recently emplaced continental calc-alkaline rocks in continental arcs [*Mantle and Collins*, 2008; *Chiaradia*, 2015; *Chapman et al*., 2015; *Profeta et al*., 2015]. However, whether this correlation was present in syncollisional to postcollisional settings has not yet been tested [*Profeta et al*., 2015], making it equivocal to track crustal thickness using geochemical indices of samples from such settings. This is the case for the $<$55 Ma samples from the Gangdese Batholith, if an India-Asia collision age of approximately 60–55 Ma is accepted [e.g., *Najman et al*., 2010; *Zhu et al*., 2015; *Hu et al*., 2016], or by the $<$34 Ma samples, if a collision age of 34–20 Ma is favored [*Aitchison et al*., 2007; *van Hinsbergen et al*., 2012].

The Ce/Y ratio of arc basalts [*Mantle and Collins*, 2008] and the La/Yb and Sr/Y ratios of arc intermediate rocks [*Chiaradia*, 2015; *Chapman et al*., 2015; *Profeta et al*., 2015] reflect intrinsically the presence of mineral assemblages (amphibole + plagioclase $\pm$ garnet) in the magma source region. When slab-derived and fractionated samples are excluded, these ratios are indicative of changing crustal thickness [e.g., *Mantle and Collins*, 2008; *Chiaradia*, 2015; *Chapman et al*., 2015; *Profeta et al*., 2015]. Such understanding, along with thickened lower crust-derived geochemical signatures of the 50–10 Ma samples from the Gangdese Batholith [*Chung et al*., 2003, 2009; *Ji et al*., 2012; *Guan et al*., 2012; *Q. Wang et al*., 2015], enables us to extend the approach of

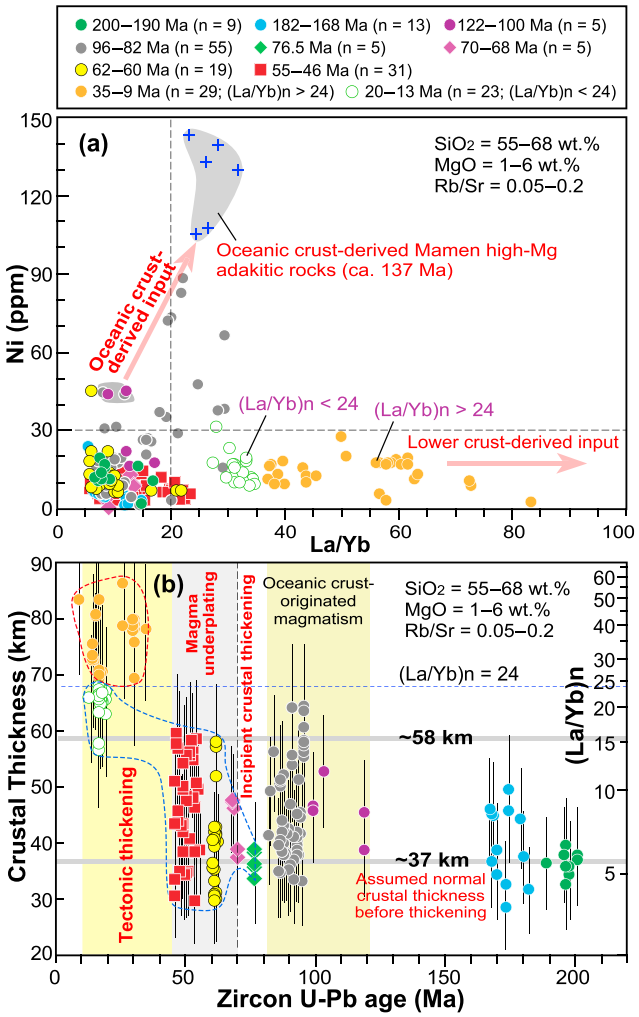

Figure 3. (a) Plot of La/Yb ratio versus Ni abundance (ppm) for the intermediate intrusive rocks (85–94°E) from the Gangdese arc in southern Tibet. Data of the approximately 137 Ma oceanic crust-derived Mamen high-Mg adakitic rocks are from *Zhu et al.* [2009]. (b) Plot of changes in (La/Yb)n (*n* denotes the normalized to chondritic values of *McDonough and Sun* [1995]) in intrusive rocks and calculated crustal thickness over time for the Gangdese arc. Crustal thickness with uncertainty is calculated following the method of *Profeta et al.* [2015] (see the supporting information). Note that the 122–82 Ma samples that are inferred to have originated from the subducting Neo-Tethyan oceanic crust and some 35–9 Ma samples with high (La/Yb)n (>24) that are not constrained to a geophysically determined Moho depth [*Profeta et al.*, 2015] are not used in the crustal thickness discussions. See text for details.

Profeta et al. [2015], which is established from continental arc magmatism, to all filtered intermediate samples in quantifying the spatial and temporal variations in crustal thickness of the Gangdese arc. Indeed, such an extended application has been verified by modern collisional magmas in the Carpathians and Caucasus (Mihai N. Ducea, personal communication, 2016).

The empirical fit defined by the La/Yb ratios of global intermediate rocks with crustal thickness [*Profeta et al.*, 2015] is used to track the crustal thickness of the Gangdese arc in southern Tibet. This is because (1) the basaltic rocks that are available for the approach of *Mantle and Collins* [2008] are rare in the arc and (2) some intermediate rocks show very high Sr/Y ratios (>100) that are greater than expected for differentiation within even the thickest crust based on global compilations [*Chapman et al.*, 2015]. (La/Yb)n (n denotes normalized to chondritic values of *McDonough and Sun* [1995]) and calculated crustal thickness, following the method of *Profeta et al.* [2015], for the intermediate intrusive rocks (55–68 wt % SiO_2) from the Gangdese Batholith are plotted against age in Figure 3b. A first-order observation is that calculated crustal thickness increases at approximately 70 Ma and becomes high but relatively constant from approximately 60 Ma to 45 Ma and then displays a further increase after 30 Ma (Figure 3b). Samples in the age range of 122–82 Ma that are inferred to have originated from the subducting Neo-Tethyan oceanic crust and some samples between 35 and 9 Ma, which show very high (La/Yb)n (>24) and hence are not constrained to a geophysically determined Moho depth [*Profeta et al.*, 2015], are not used in the crustal thickness discussions.

4. Discussions

4.1. Quantifying the Crustal Thickness of the Gangdese Arc Over Time

Mantle and Collins [2008] show that the maximum Ce/Y of arc basalt from major arc systems on the Earth increases with the depth of the local Moho, and they apply this to infer changes in crustal thickness of the New Zealand region since 400 Ma. Subsequent work validates the maximum values of thickened crust-indicated geochemical indices (e.g., high Sr/Y, La/Yb, and Sm/Yb) in tracking the extent of crustal thickening in the central Andes over time [*Mamani et al.*, 2010]. The evolving maximum (La/Yb)n ratios based on the data

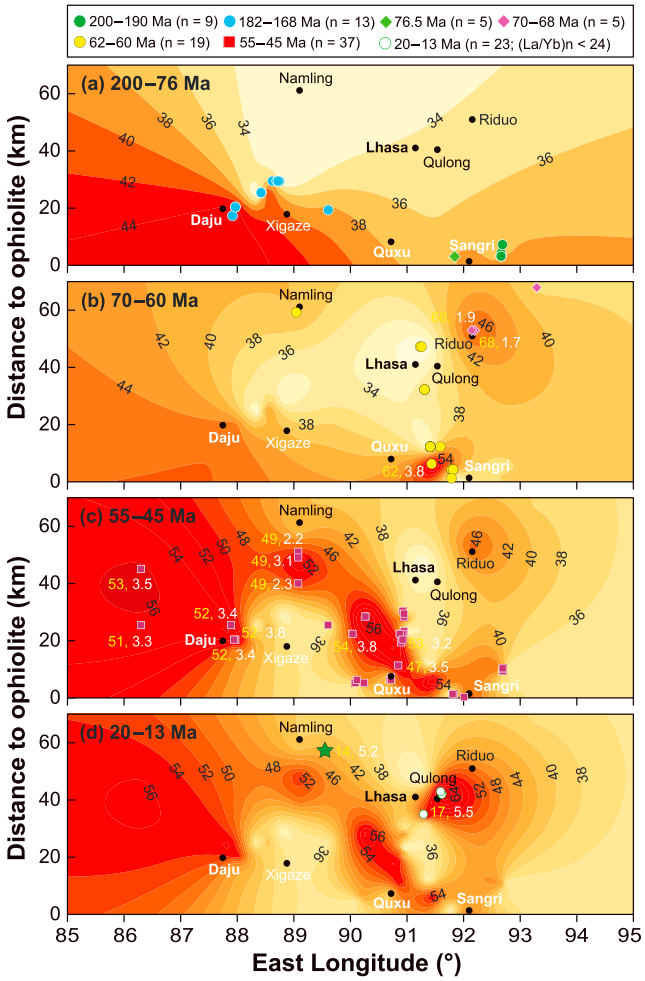

Figure 4. Contour plots of crustal thickness and reconstructed paleoelevation of the Gangdese arc at (a) approximately 200–76 Ma, (b) approximately 70–60 Ma, (c) approximately 55–45 Ma, and (d) approximately 20–13 Ma. The symbols with numerals denote the crystallization age (in yellow) and paleoelevation (in white), respectively. Paleoelevation data: SE Namling [*Currie et al.*, 2005]. These figures are generated by Di-Cheng Zhu, using Surfer version 10.3.705 created by Golden Software, Inc., under an open license.

currently available indicate that the Gangdese crust was likely of normal thickness prior to approximately 70 Ma (~37 km; Figures 3b and 4a) but has been thickened locally to 47 ± 9 km at approximately 70 Ma (e.g., Riduo) and to 58 ± 10 km at approximately 60 Ma (e.g., west of Sangri; Figure 4b) and then more broadly to (58–50) ± 10 km at 55–45 Ma from north of Quxu to west of Daju extending over 400 km along the strike of the arc (Figure 4c). Such an early age of crustal thickening (60–45 Ma) is in broad agreement with the timing of thickening based on the presence of adakitic rocks in Naika (approximately 62 Ma) [*Jiang et al.*, 2014], Linzhou (52.5 Ma) [*Mo et al.*, 2007; *Zhu et al.*, 2015], and Niedang (approximately 51 Ma) [*Ji et al.*, 2012] from the Gangdese Batholith and the results of structural relationships in Dala (>44 Ma) [*Aikman et al.*, 2008] from the Tethyan Himalaya (Figure 1b).

Our data also suggest that the crust beneath Qulong has been thickened to 68 ± 12 km at 20–10 Ma (Figure 4d), further corroborating the presence of a thickened crust (>50 km) beneath the Gangdese arc between 30 Ma and 9 Ma [*Chung et al.*, 2003, 2009].

4.2. Mechanisms for Crustal Thickening of the Gangdese Arc Over Time

Structural geology studies reveal that the hinterland portion of the Lhasa Terrane (i.e., north of the Gangdese arc; Figure 1b) may have attained an Andean-style thick crust due to widespread folding and thrust faulting during the Cretaceous (>99 Ma [*Murphy et al.*, 1997] and 90–69 Ma [*Kapp et al.*, 2007]). Similar tectonic shortening may be invoked to account for crustal thickening of the Gangdese arc during 55–45 Ma as indicated by (1) the shift in the whole-rock Nd and zircon Hf isotopic compositions toward negative values at approximately 50 Ma that is interpreted to reflect the involvement of the Indian crust-derived materials in the generation of the Gangdese Batholith after approximately 50 Ma [e.g., *Zhu et al.*, 2015], (2) the Tethyan Himalayan folding and thrusting (Figure 1b) that was likely active during 55–45 Ma [*Ratschbacher et al.*, 1994; *Aikman et al.*, 2008; *Smit et al.*, 2014], and (3) the medium-pressure metamorphism in Dala from the Tethyan Himalaya that suggests the presence of the upper Indian crust at depths of 20–30 km beneath the Gangdese arc during 48–45 Ma [*Ding et al.*, 2016].

However, we consider that tectonic shortening may not be the major cause for the early stage of crustal thickening (60–45 Ma) of the Gangdese arc as the arc has broadly thickened to (58–50) ± 10 km prior to approximately 50 Ma (Figure 4c). Major geological constraints for this argument include the following: (1) the strong folding and deformation prior to approximately 50 Ma (i.e., during 105–69 Ma) that occurred in the southern margin of the hinterland Lhasa Terrane along the Emei La–Gulu thrust (including the angular unconformity in

Coqin, Maqu, and Linzhou; Figure 1b) rather than the Gangdese arc [*Murphy et al*., 1997; *Kapp et al*., 2007]; (2) the early Tertiary Linzizong volcanic sequence in the Lhasa Terrane (60–52 Ma) [*Zhu et al*., 2015] is weakly deformed [e.g., *Murphy et al*., 1997; *Mo et al*., 2007; *Kapp et al*., 2007]; and (3) there is no direct evidence for contraction between 69 and 53 Ma [*Kapp et al*., 2007], and the amount of inferred crustal shortening along the south Lhasa thrust within the Gangdese Batholith during this period (Figure 1b) is small [e.g., *Harrison et al*., 1992; *Kapp et al*., 2007].

Instead, field observations and geochronological data indicate that the Gangdese crust may have experienced significant basaltic magma underplating at 60–45 Ma [*Dong et al*., 2005; *Mo et al*., 2005]. This is inferred to be geodynamically associated with the rollback of the Neo-Tethyan oceanic lithosphere from approximately 70 Ma followed by slab breakoff at approximately 53 Ma, which is capable of inducing basaltic magmatism over several million years [*van de Zedde and Wortel*, 2001]. These interpretations are supported by the southward migration of the magmatism from 72–65 Ma to 64–48 Ma, widely developed mafic enclaves and dykes at approximately 53–47 Ma, significantly increased zircon saturation temperature at approximately 52 Ma, peak magmatic activity at approximately 51 Ma [*Zhu et al*., 2015; *R. Wang et al*., 2015] documented in the Gangdese Batholith, and oceanic island basalt-type magmatism at approximately 45 Ma in the Tethyan Himalaya [*Ji et al*., 2016]. Available data summarized here appear to indicate that the initiation of crustal thickening (approximately 70 Ma; Figure 3b) corresponds with the onset of increased mantle input [*Zhu et al*., 2015]. This synchronicity suggests that the crustal thickening of the Gangdese arc during 70–45 Ma is largely the consequence of basaltic magma underplating as a result of slab rollback and slab breakoff [*Yin and Harrison*, 2000; *Mo et al*., 2007; *Zhu et al*., 2015]. Given a normal starting average thickness of ~37 km (Figure 3b), underplating may have thickened the Gangdese crust ~20 km to ~58 km. Such a value is some 5 km thicker than the previous estimate of magmatic addition (~15 km), which was based on seismic data [*Mo et al*., 2007].

Gangdese arc magmatism in the period of 60–45 Ma was followed by magmatic lulls at 40–20 Ma and 10–0 Ma (Figure 2), separated by volumetrically small but widespread felsic-dominated plutonism at 20–10 Ma, indicating that mafic magmatic addition has contributed little to crustal thickening since 40 Ma. In contrast, the additional ~20 km of crustal thickening from 40 Ma to the present day, which is divisible into an increase from 58 ± 10 km to 68 ± 12 km between 40 and 10 Ma (Figure 3b) and from 68 ± 12 km to 75–80 km [*Jiménez-Munt et al*., 2008] since 10 Ma, can be attributed to tectonic thickening due to intracontinental thrusting and underplating of the lower Indian crust since 40 Ma [*Chung et al*., 2009]. Evidence for this interpretation include (1) the movement along the Gangdese thrust at 30–24 Ma and the Great Counter thrust at 19–10 Ma (Figure 1b) [*Yin et al*., 1994, 1999]; (2) the presence of approximately 30 Ma adakitic rocks and approximately 35 Ma gabbros with negative whole-rock $\varepsilon_{Nd}(t)$ from the Gangdese Batholith that are interpreted to originate from northward subduction of the lower Indian crust [*Jiang et al*., 2014] and lithospheric mantle metasomatized by subducted Indian continental sediments [*Ma et al*., 2017], respectively; and (3) the observation of a 15 km thick strong velocity-depth gradient layer above the Moho in the southern Lhasa Terrane, which suggests the underplating of lower Indian crust developed since 25–20 Ma [*Nábělek et al*., 2009].

4.3. Insights into the Uplift of the Gangdese Mountains

Previous studies on sedimentary facies and structural relationships from the hinterland portion of the Lhasa Terrane suggest the presence of an elevated Andean-type margin (perhaps ~4000 m) by the end of the Cretaceous (>69 Ma) [e.g., *England and Searle*, 1986; *Murphy et al*., 1997; *Kapp et al*., 2007]. However, the elevation history of the Gangdese arc within an evolving space-time framework remains unconstrained.

If the height of the southern Tibetan Plateau is compensated isostatically by crustal thickening [e.g., *England and Searle*, 1986; *Molnar et al*., 1993; *Jiménez-Munt et al*., 2008], the changing thickness outlined in Figure 3b requires changes in the elevation of the Gangdese arc over time. Given an average crustal density of 2.77 g/cm^3 and an average mantle density of 3.27 g/cm^3 [*He et al*., 2014] as well as an average normal crustal thickness of ~37 km before thickening (Figure 3b), and assuming Airy isostatic compensation, our data indicate that the Gangdese arc would have locally attained elevations of 3800 ± 700 m at approximately 60 Ma (Figure 4b and Table A2 in the supporting information), which became broader at approximately 55–45 Ma, extending from west of Daju to Sangri (Figure 4c), and reached 5500 ± 900 m at 20–10 Ma at Qulong (Figure 4d and Table A2).

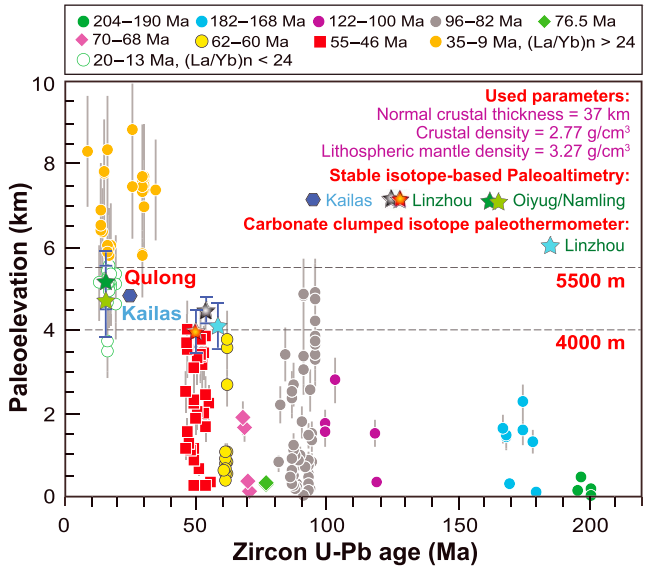

Figure 5. Plot of paleoelevation with uncertainty calculated assuming Airy isostatic compensation (see the supporting information) versus zircon U-Pb age (Ma) for the intrusive rocks (85–95°E) from the Gangdese arc. Used average crustal density of 2.77 g/cm^3 and mantle density of 3.27 g/cm^3 are from *He et al.* [2014], and normal crustal thickness (before thickening) of ~37 km is calculated from the approximately 194 Ma and 77 Ma intermediate intrusive rocks (Figure 3b). Paleoelevation data: Kailas [*DeCelles et al.*, 2011], Linzhou [*Ding et al.*, 2014; *Rowley et al.*, 2015], and Oiyug/Namling [*Spicer et al.*, 2003; *Currie et al.*, 2005].

The paleoelevation of 3800 ± 700 m at 60–45 Ma is in broad agreement with the results of the clumped isotope paleothermometer (>4100 ± 550 m) [*Rowley et al.*, 2015] and of C–O isotopic data that suggest elevations of 4500 ± 400 m at approximately 54 Ma (this age is calibrated following *Zhu et al.* [2015]) and 4000 ± 500 m at approximately 50 Ma [*Ding et al.*, 2014] from Linzhou (Figure 5). Indeed, our paleoelevation value is calculated solely from isostatic compensation and is likely an underestimate. This is because (1) the surface uplift of mountain belts largely reflects the combined effects of crustal thickening and mantle dynamic processes (e.g., lithospheric delamination or slab breakoff) [e.g., *Molnar et al.*, 1993; *von Blanckenburg and Davies*, 1995] and (2) geological, geochronological, and geochemical data indicate breakoff of the downgoing Neo-Tethyan oceanic slab, most likely occurred at approximately 53 Ma [*Zhu et al.*, 2015], which would result in surface uplift of the overriding plate [*von Blanckenburg and Davies*, 1995]. Given initial India-Asia collision that occurred at 60–55 Ma [e.g., *Zhu et al.*, 2015; *Hu et al.*, 2016], our results indicate that the Gangdese Mountains in the southern Lhasa Terrane did not resemble the hinterland Lhasa Terrane north of the Gangdese arc and the present-day central Andes in elevation before its collision with India and only attained this elevation (>4000 m) synchronous with, or shortly after, collision.

Our results suggest that the Qulong region was likely uplifted to 5500 ± 900 m (as high as today) at 20–10 Ma (Figure 4d and Table A2), in agreement with paleoelevations reconstructed by oxygen isotopic data of pedogenic, early diagenetic carbonates, and lacustrine-siderite from Oiyug (5200 + 1370/−605 m [*Currie et al.*, 2005] and 5.1 km + 1.3/−1.9 km [*Currie et al.*, 2016]), fossil leaf assemblages from Namling (4689 ± 895 m) [*Spicer et al.*, 2003], and oxygen isotopic data of paleosol carbonates from Kailas (>4700 m) [*DeCelles et al.*, 2011] (Figures 1b and 5). These similar paleoelevation estimates suggest that (1) the entire Gangdese Mountains (Figure 1b) was at high elevation (5000 ± 500 m) by 20–10 Ma and (2) uplift at this time can be explained by isostatic compensation, and hence, models invoking removal of lower lithosphere [*Molnar et al.*, 1993] are not needed to drive uplift. Indeed, the Gangdese crust did not appear to have undergone any thinning since 60 Ma (Figure 3b), which is inconsistent with the prediction that delamination would thin the crust [*Mamani et al.*, 2010].

5. Broader Implications

Our results indicate that the crust of the Lhasa Terrane beneath the Gangdese magmatic arc has been thickened to 58–50 km at 55–45 Ma, covering a broad region over 400 km along strike (Figure 4c). If Airy isostatic compensation applied, this thick crust suggests that an elevation of >4000 m would have existed along the Gangdese Mountains at that period. This paleoelevation estimate coincides not only with the C–O isotope-based paleoaltimetry [*Ding et al.*, 2014] but also with the carbonate-clumped isotope paleothermometer [*Rowley et al.*, 2015]. The Gangdese case presented here is analogous to that described for the Sevier hinterland in western North America, where a thick crust (60–50 km thick) by the end of Mesozoic is used to infer isostatically the presence of a high-elevation plateau of >2 km (more likely >3 km) (i.e., Nevadaplano) [*Coney*

and Harms, 1984; *DeCelles*, 2004; *DeCelles and Coogan*, 2006], and verified by carbonate-clumped isotope thermometry [*Snell et al*., 2014]. In some cases, elevation does not correlate with crustal thickness as seen in the Altiplano-Puna Plateau of the central Andes, which is interpreted as the consequence of the presence of dense eclogitic lower crust that can drag the surface down [*Garzione et al*., 2008]. Such a case may also exist in the Gangdese Mountains but needs more data and further effort to justify.

We note that our paleoelevation estimates of Airy isostatic compensation for the Gangdese Mountains are based on calculations of crustal thickness following an empirical fit [*Profeta et al*., 2015]. This approach includes inherent uncertainties of crustal thickness (Figure 3b) (see the supporting information for the uncertainty calculation), potential sampling bias, and uncertainties of crustal and mantle densities that may contain lateral heterogeneities [*He et al*., 2014]. Nevertheless, our results demonstrate that when parameters used for Airy isostatic calculation (including normal crustal thickness and crustal and mantle densities) are geologically reasonable, based on local geophysical data, the paleoelevations obtained from magmatic compositions are indeed comparable to those of stable isotope-based paleoaltimetry. This comparability implies that intermediate rocks with distinct geochemistry from convergent margins can be used as an alternative proxy that contains evolving space-time information to reconstruct paleoelevation for ancient orogens.

Acknowledgments

Constructive comments on an earlier draft of the manuscript by An Yin, Paul Kapp, Mihai Ducea, Peter Copeland, Ling Chen, Yaoling Niu, Xiumian Hu, Sheng-Ao Liu, and Ya-Lin Li are gratefully acknowledged. This research was financially supported by the National Science Foundation of China (41225006 and 41472061), and the MOST of China (2016YFC0600304 and 2016YFC0600407), the Strategic Priority Research Program (B) of the Chinese Academy of Sciences (XDB03010301), and the MOST Special Fund from the State Key Laboratory of Geological Processes and Mineral Resources (China University of Geosciences). The data for this paper are available by contacting the corresponding author (dchengzhu@163.com). Constructive reviews and suggestions by two anonymous reviewers and Editor Michael Walter helped us to further improve the manuscript. This is CUGB petro-geochemical contribution PGC-201519.

References

Aikman, A. B., T. M. Harrison, and L. Ding (2008), Evidence for early (>44 Ma) Himalayan crustal thickening, Tethyan Himalaya, southeastern Tibet, *Earth Planet. Sci. Lett.*, *274*, 14–23.

Aitchison, J. C., J. R. Ali, and A. M. Davis (2007), When and where did India and Asia collide, *J. Geophys. Res.*, *112*, B05423, doi:10.1029/2006JB004706.

Chapman, J. B., M. N. Ducea, P. G. DeCelles, and L. Profeta (2015), Tracking changes in crustal thickness during orogenic evolution with Sr/Y: An example from the North American Cordillera, *Geology*, *43*, 919–922.

Chiaradia, M. (2015), Crustal thickness control on Sr/Y signatures of recent arc magmas: An Earth scale perspective, *Sci. Rep.*, *5*, 8115, doi:10.1038/srep08115.

Chung, S. L., D. Y. Liu, J. Q. Ji, M. F. Chu, H. Y. Lee, D. J. Wen, C. H. Lo, T. Y. Lee, Q. Qian, and Q. Zhang (2003), Adakites from continental collision zones: Melting of thickened lower crust beneath southern Tibet, *Geology*, *31*, 1021–1024.

Chung, S. L., M. F. Chu, Y. Q. Zhang, Y. W. Xie, C. H. Lo, T. Y. Lee, C. Y. Lan, X. H. Li, Q. Zhang, and Y. Z. Wang (2005), Tibetan tectonic evolution inferred from spatial and temporal variations in post-collisional magmatism, *Earth Sci. Rev.*, *68*, 173–196.

Chung, S. L., M. F. Chu, J. Q. Ji, S. Y. O'Reilly, N. J. Pearson, D. Y. Liu, T. Y. Lee, and C. H. Lo (2009), The nature and timing of crustal thickening in southern Tibet: Geochemical and zircon Hf isotopic constraints from postcollisional adakites, *Tectonophysics*, *477*, 36–48.

Coney, P. J., and T. A. Harms (1984), Cordilleran metamorphic core complexes—Cenozoic extensional relics of Mesozoic compression, *Geology*, *12*, 550–554.

Copeland, P., T. M. Harrison, Y. Pan, W. S. F. Kidd, M. Roden, and Y. Zhang (1995), Thermal evolution of the Gangdese Batholith, southern Tibet: A history of episodic unroofing, *Tectonics*, *14*, 223–226, doi:10.1029/94TC01676.

Currie, B. S., D. B. Rowley, and N. J. Tabor (2005), Middle Miocene paleoaltimetry of southern Tibet: Implications for the role of mantle thickening and delamination in the Himalayan orogen, *Geology*, *33*, 181–184.

Currie, B. S., P. J. Polissar, D. B. Rowley, M. Ingalls, S. Li, G. Olack, and K. H. Freeman (2016), Multiproxy paleoaltimetry of the late Oligocene-Pliocene Oiyug Basin, southern Tibet, *Am. J. Sci.*, *316*, 401−436.

DeCelles, P. G. (2004), Late Jurassic to Eocene evolution of the Cordilleran thrust belt and foreland basin system, western USA, *Am. J. Sci.*, *304*, 105–168.

DeCelles, P. G., and J. C. Coogan (2006), Regional structure and kinematic history of the Sevier fold-and-thrust belt, central Utah, *Geol. Soc. Am. Bull.*, *118*, 841–864.

DeCelles, P. G., P. Kapp, J. Quade, and G. E. Gehrels (2011), Oligocene–Miocene Kailas basin, southwestern Tibet: Record of postcollisional upper-plate extension in the Indus-Yarlung suture zone, *Geol. Soc. Am. Bull.*, *123*, 1337–1362.

Defant, M. J., and M. S. Drummond (1990), Derivation of some modern arc magmas by melting of young subducted lithosphere, *Nature*, *347*, 662–665.

Ding, H. X., Z. M. Zhang, X. Dong, Z. L. Tian, H. Xiang, H. C. Mu, Z. B. Gou, X. F. Shui, W. C. Li, and L. J. Mao (2016), Early Eocene (c. 50 Ma) collision of the Indian and Asian continents: Constraints from the North Himalayan metamorphic rocks, southeastern Tibet, *Earth Planet. Sci. Lett.*, *435*, 64–73.

Ding, L., Q. Xu, Y. H. Yue, H. Q. Wang, F. L. Cai, and S. Li (2014), The Andean-type Gangdese Mountains: Paleoelevation record from the Paleocene–Eocene Linzhou Basin, *Earth Planet. Sci. Lett.*, *392*, 250–264.

Dong, G. C., X. X. Mo, Z. D. Zhao, T. Y. Guo, L. L. Wang, and T. Chen (2005), Geochronologic constraints on the magmatic underplating of the Gangdise belt in the India–Eurasia collision: Evidence of SHRIMP II zircon U–Pb dating, *Acta Geol. Sin.*, *79*, 787–794.

England, P. C., and M. Searle (1986), The Cretaceous-Tertiary deformation of the Lhasa block and its implications for crustal thickening in Tibet, *Tectonics*, *5*, 1–14, doi:10.1029/TC005i001p00001.

Garzione, C. N., G. D. Hoke, J. C. Libarkin, S. Withers, B. MacFadden, J. Eiler, P. Ghosh, and A. Mulch (2008), Rise of the Andes, *Science*, *320*, 1304–1307.

Guan, Q., et al. (2012), Crustal thickening prior to 38 Ma in southern Tibet: Evidence from lower crust-derived adakitic magmatism in the Gangdese Batholith, *Gondwana Res.*, *21*, 88–99.

Harrison, T. M., P. Copeland, W. S. F. Kidd, and A. Yin (1992), Raising Tibet, *Science*, *255*, 1663–1670.

Haschke, M., W. Siebel, A. Günther, and E. Scheuber (2002), Repeated crustal thickening and recycling during the Andean orogeny in north Chile (21°–26°S), *J. Geophys. Res.*, *107*, doi:10.1029/2001JB000328.

He, R. Z., G. C. Liu, E. Golos, R. Gao, and H. W. Zheng (2014), Isostatic gravity anomaly, lithospheric scale density structure of the northern Tibetan Plateau and geodynamic causes for potassic lava eruption in Neogene, *Tectonophysics*, *628*, 218–227.

Hu, X. M., E. Garzanti, J. G. Wang, W. T. Huang, W. An, and A. Webb (2016), The timing of India-Asia collision onset—Facts, theories, controversies, *Earth Sci. Rev.*, *160*, 264–299.
Ji, W. Q., F. Y. Wu, C. Z. Liu, and S. L. Chung (2012), Early Eocene crustal thickening in southern Tibet: New age and geochemical constraints from the Gangdese Batholith, *J. Asian Earth Sci.*, *53*, 82–95.
Ji, W. Q., F. Y. Wu, S. L. Chung, J. X. Li, and C. Z. Liu (2009), Zircon U–Pb chronology and Hf isotopic constraints on the petrogenesis of Gangdese batholiths, southern Tibet, *Chem. Geol.*, *262*, 229–245.
Ji, W. Q., F. Y. Wu, S. L. Chung, X. C. Wang, C. Z. Liu, Q. L. Li, Z. C. Liu, X. C. Liu, and J. G. Wang (2016), Eocene Neo-Tethyan slab breakoff constrained by 45 Ma oceanic island basalt-type magmatism in southern Tibet, *Geology*, *44*, 283–286.
Jiang, Z. Q., et al. (2014), Transition from oceanic to continental lithosphere subduction in southern Tibet: Evidence from the Late Cretaceous–Early Oligocene (~91–30 Ma) intrusive rocks in the Chanang–Zedong area, southern Gangdese, *Lithos*, *196–197*, 213–231.
Jiménez-Munt, I., M. Fernàndez, J. Vergés, and J. P. Platt (2008), Lithosphere structure underneath the Tibetan Plateau inferred from elevation, gravity and geoid anomalies, *Earth Planet. Sci. Lett.*, *267*, 276–289.
Kapp, P., P. G. DeCelles, A. L. Leier, J. M. Fabijanic, S. He, A. Pullen, G. E. Gehrels, and L. Ding (2007), The Gangdese retroarc thrust belt revealed, *GSA Today*, *17*, 4–9.
Ma, L., Q. Wang, D. A. Wyman, Z. X. Li, Z. Q. Jiang, J. H. Yang, G. N. Gou, and H. F. Guo (2013), Late Cretaceous (100–89 Ma) magnesian charnockites with adakitic affinities in the Milin area, eastern Gangdese: Partial melting of subducted oceanic crust and implications for crustal growth in southern Tibet, *Lithos*, *175–176*, 315–332.
Ma, L., Q. Wang, Z. X. Li, D. A. Wyman, J. H. Yang, Z. Q. Jiang, Y. S. Liu, G. L. Gou, and H. F. Guo (2017), Subduction of Indian continent beneath southern Tibet in the latest Eocene (~35 Ma): Insights from the Quguosha gabbros in southern Lhasa block, *Gondwana Res.*, *41*, 77–92.
Mamani, M., G. Wörner, and T. Sempere (2010), Geochemical variations in igneous rocks of the central Andean orocline (13°S to 18°S): Tracing crustal thickening and magma generation through time and space, *Geol. Soc. Am. Bull.*, *122*, 162–182.
Mantle, G. W., and W. J. Collins (2008), Quantifying crustal thickness variations in evolving orogens: Correlation between arc basalt composition and Moho depth, *Geology*, *36*, 87–90.
Martin, H., R. H. Smithies, R. Rapp, J. F. Moyen, and D. Champion (2005), An overview of adakite, tonalite-trondhjemite-granodiorite (TTG), and sanukitoid: Relationships and some implications for crustal evolution, *Lithos*, *79*, 1–24.
McDonough, W. F., and S. S. Sun (1995), The composition of the Earth, *Chem. Geol.*, *120*, 223–253.
Mo, X. X., G. C. Dong, Z. D. Zhao, T. Y. Guo, L. L. Wang, and T. Chen (2005), Timing of magma mixing in the Gangdise magmatic belt during the India–Asia collision: Zircon SHRIMP U–Pb dating, *Acta Geol. Sin.*, *79*, 66–76.
Mo, X. X., Z. Q. Hou, Y. L. Niu, G. C. Dong, X. M. Qu, Z. D. Zhao, and Z. M. Yang (2007), Mantle contributions to crustal thickening during continental collision: Evidence from Cenozoic igneous rocks in southern Tibet, *Lithos*, *96*, 225–242.
Molnar, P., P. England, and J. Martinod (1993), Mantle dynamics, uplift of the Tibetan Plateau, and the Indian monsoon, *Rev. Geophys.*, *31*, 357–396, doi:10.1029/93RG02030.
Murphy, M. A., A. Yin, T. M. Harrison, S. B. Durr, Z. Chen, F. J. Ryerson, W. S. F. Kidd, X. Wang, and X. Zhou (1997), Did the Indo-Asian collision alone create the Tibetan Plateau, *Geology*, *25*, 719–722.
Nábělek, J., G. Hetenyi, J. Vergne, S. Sapkota, B. Kafle, M. Jiang, H. Su, J. Chen, B. S. Huang, and H.-C. L. I. M. B. Team (2009), Underplating in the Himalaya-Tibet collision zone revealed by the Hi-CLIMB experiment, *Science*, *325*, 1371–1374.
Najman, Y., E. Appel, M. Boudagher-Fadel, P. Bown, A. Carter, E. Garzanti, L. Godin, J. Han, U. Liebke, and G. Oliver (2010), Timing of India–Asia collision: Geological, biostratigraphic, and palaeomagnetic constraints, *J. Geophys. Res.*, *115*, B12416, doi:10.1029/2010JB007673.
Plank, T., and C. H. Langmuir (1988), An evaluation of the global variations in the major element chemistry of arc basalts, *Earth Planet. Sci. Lett.*, *90*, 349–370.
Profeta, L., M. N. Ducea, J. B. Chapman, S. R. Paterson, S. M. Henriquez Gonzales, M. Kirsch, L. Petrescu, and P. G. DeCelles (2015), Quantifying crustal thickness over time in magmatic arcs, *Sci. Rep.*, *5*, 17,786, doi:10.1038/srep17786.
Rapp, R. P., N. Shimizu, M. D. Norman, and G. S. Applegate (1999), Reaction between slab-derived melts and peridotite in the mantle wedge: Experimental constraints at 3.8 GPa, *Chem. Geol.*, *160*, 335–356.
Ratschbacher, L., W. Frisch, G. Liu, and C. C. Chen (1994), Distributed deformation in southern and western Tibet during and after the India-Asian collision, *J. Geophys. Res.*, *99*, 19,917–19,945, doi:10.1029/94JB00932.
Rowley, D. B., M. Ingalls, A. S. Colman, B. Currie, S. Y. Li, G. Olack, and L. Ding (2015), ~55 Ma aged high topography of the Lhasa Block from stable and clumped isotope paleoaltimetry: Implications for ~50 ± 25% crustal mass deficit in the India-Asia collisional system, Abstract of AGU Fall Meeting, San Francisco, No. T12B-06.
Smit, M. A., B. R. Hacker, and J. Lee (2014), Tibetan garnet records early Eocene initiation of thickening in the Himalaya, *Geology*, *42*, 591–594.
Snell, K. E., P. L. Koch, P. Druschke, B. Z. Foreman, and J. M. Eiler (2014), High elevation of the "Nevadaplano" during the Late Cretaceous, *Earth Planet. Sci. Lett.*, *386*, 52–63.
Spicer, R. A., N. B. W. Harris, M. Widdowson, A. B. Herman, S. Guo, P. J. Valdes, J. A. Wolfe, and S. P. Kelley (2003), Constant elevation of southern Tibet over the past 15 million years, *Nature*, *421*, 622–624.
van de Zedde, D. M. A., and M. J. R. Wortel (2001), Shallow slab detachment as a transient source of heat at midlithospheric depth, *Tectonics*, *20*, 868–882, doi:10.1029/2001TC900018.
van Hinsbergen, D. J. J., P. C. Lippert, G. Dupont-Nivet, N. McQuarrie, P. V. Doubrovine, W. Spakman, and T. H. Torsvik (2012), Greater India Basin hypothesis and a two-stage Cenozoic collision between India and Asia, *Proc. Natl. Acad. Sci. U.S.A.*, *109*, 7659–7664, doi:10.1073/pnas.1117262109.
von Blanckenburg, F., and J. H. Davies (1995), Slab breakoff: A model for syncollisional magmatism and tectonics in the Alps, *Tectonics*, *14*, 120–131, doi:10.1029/94TC02051.
Wang, C. S., X. X. Zhao, Z. F. Liu, P. C. Lippert, S. A. Graham, R. S. Coe, H. S. Yi, L. D. Zhu, S. Liu, and Y. L. Li (2008), Constraints on the early uplift history of the Tibetan Plateau, *Proc. Natl. Acad. Sci. U.S.A.*, *105*, 4987–4992.
Wang, Q., D. C. Zhu, P. A. Cawood, Z. D. Zhao, S. A. Liu, S. L. Chung, L. L. Zhang, D. Liu, Y. C. Zheng, and J. G. Dai (2015), Eocene magmatic processes and crustal thickening in southern Tibet: Insights from strongly fractionated ca. 43 Ma granites in the western Gangdese Batholith, *Lithos*, *239*, 128–141.
Wang, R., J. P. Richards, Z. Q. Hou, F. An, and R. A. Creaser (2015), Zircon U–Pb age and Sr–Nd–Hf–O isotope geochemistry of the Paleocene–Eocene igneous rocks in western Gangdese: Evidence for the timing of Neo-Tethyan slab breakoff, *Lithos*, *224–225*, 179–194.
Yakovlev, P. V., and M. K. Clark (2014), Conservation and redistribution of crust during the Indo-Asian collision, *Tectonics*, *33*, 1016–1027, doi:10.1002/2013TC003469.
Yin, A., and T. M. Harrison (2000), Geologic evolution of the Himalayan–Tibetan orogen, *Annu. Rev. Earth Planet. Sci.*, *28*, 211–280.

Yin, A., T. M. Harrison, F. J. Ryerson, W. Chen, W. S. F. Kidd, and P. Copeland (1994), Tertiary structural evolution of the Gangdese thrust system, southeastern Tibet, *J. Geophys. Res.*, *99*, 18,175–18,201, doi:10.1029/94JB00504.

Yin, A., T. M. Harrison, M. A. Murphy, M. Grove, S. Nie, F. J. Ryerson, W. X. Feng, and C. Z. Le (1999), Tertiary deformation history of southeastern and southwestern Tibet during the Indo-Asian collision, *Geol. Soc. Am. Bull.*, *111*, 1644–1664.

Zhu, D. C., Z. D. Zhao, Y. L. Niu, X. X. Mo, S. L. Chung, Z. Q. Hou, L. Q. Wang, and F. Y. Wu (2011), The Lhasa Terrane: Record of a microcontinent and its histories of drift and growth, *Earth Planet. Sci. Lett.*, *301*, 241–255.

Zhu, D. C., Z. D. Zhao, Y. L. Niu, Y. Dilek, Z. Q. Hou, and X. X. Mo (2013), The origin and pre-Cenozoic evolution of the Tibetan Plateau, *Gondwana Res.*, *23*, 1429–1454.

Zhu, D. C., Q. Wang, Z. D. Zhao, S. L. Chung, P. A. Cawood, Y. L. Niu, S. A. Liu, F. Y. Wu, and X. X. Mo (2015), Magmatic record of India-Asia collision, *Sci. Rep.*, *5*, 14,289, doi:10.1038/srep14289.

Zhu, D. C., S. M. Li, P. A. Cawood, Q. Wang, Z. D. Zhao, S. A. Liu, and L. Q. Wang (2016), Assembly of the Lhasa and Qiangtang terranes in central Tibet by divergent double subduction, *Lithos*, *245*, 7–17.

Zhu, D. C., G. T. Pan, Z. D. Zhao, H. Y. Lee, Z. Q. Kang, Z. L. Liao, L. Q. Wang, G. M. Li, G. C. Dong, and B. Liu (2009), Early Cretaceous subduction-related adakite-like rocks in the Gangdese, south Tibet: Products of slab melting and subsequent melt–peridotite interaction, *J. Asian Earth Sci.*, *34*, 298–309.